

An updated calculation of the high energy diffuse gamma and neutrino flux from the galactic disk

Francesco L. Villante^{1,2}, Maddalena Cataldo^{1,2}, Giulia Pagliaroli^{2,3} and Vittoria Vecchiotti^{2,3}

¹*Department of Physical and Chemical Science (DSFC), University of L'Aquila,
L'Aquila I-67100, Italy*

²*Laboratori Nazionali del Gran Sasso (LNGS), Istituto Nazionale Fisica Nucleare (INFN),
Assergi (AQ) I-67100, Italy*

³*Gran Sasso Science Institute (GSSI),
L'Aquila I-67100, Italy*

We provide updated expectations for the diffuse gamma and neutrino emission produced in the TeV domain by the interaction of cosmic rays with the gas contained in the galactic disk. Motivated by recent analyses of the Fermi-LAT data, we consider different assumptions for the cosmic ray space and energy distribution in the Galaxy, including the possibility that cosmic ray energy spectrum depends on the galactocentric distance.

Keyword: High energy photons and neutrinos.

1. Introduction

Cosmic rays (CR) that propagate in different regions of the Galaxy interact with the gas contained in the galactic disk through hadronic processes and produce a diffuse flux of high energy (HE) gammas and neutrinos. These particles propagate to Earth along straight lines providing us with information on the CR space and energy distributions and, thus, in turn, on the CR transport in the galactic magnetic field. In this work, we present updated predictions for the diffuse galactic gamma-ray and neutrino flux produced by this mechanism in the TeV domain. Our results are obtained by using the phenomenological approach introduced in Ref. 1 that allows us to implement different assumptions for the CR space and energy distribution in a simple and direct way, including the possibility of a position dependent CR spectral index, recently emerged from analyses of the Fermi-LAT data^{2–5}.

2. The diffuse gamma and neutrino fluxes

The diffuse gamma (at energies $E_\gamma \leq 20$ TeV where gamma ray absorption in the Galactic radiation field is expected to be negligible) and neutrino fluxes produced by the interaction of CR with the interstellar medium in the galactic plane can be written as:

$$\varphi_{i,\text{diff}}(E_i, \hat{n}_i) = A_i \left[\int_{E_i}^{\infty} dE \frac{\sigma(E)}{E} F_i \left(\frac{E_i}{E}, E \right) \int_0^{\infty} dl \varphi_{\text{CR}}(E, \mathbf{r}_\odot + l \hat{n}_i) n_{\text{H}}(\mathbf{r}_\odot + l \hat{n}_i) \right], \quad (1)$$

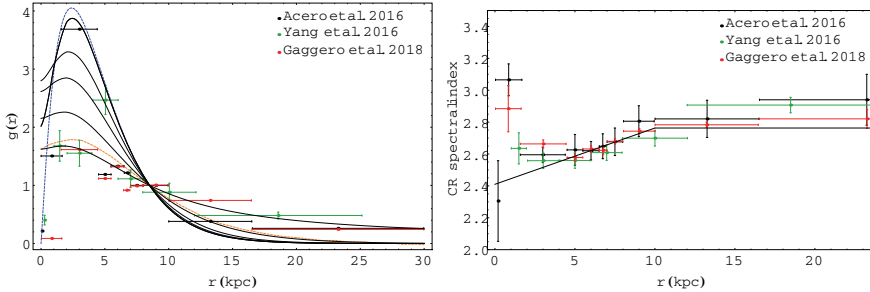


Fig. 1. Left Panel: The black lines show the functions $g(\mathbf{r})$ obtained from Eq. (5) for different smearing radii R . Going from top to bottom at $r \simeq 2$ kpc, the different lines correspond to $R = 1, 3, 5, 10, \infty$ kpc, respectively. The data points^{3–5} show the CR density at $E \simeq 20$ GeV (normalized to one at the Sun position) and the γ -ray emissivity above $E_\gamma = 1$ GeV, as a function of the galactocentric distance obtained from Fermi-LAT data. Right Panel: The black line gives the spectral index of CR at $E_{\text{CR}} = 20$ GeV adopted in this calculation. The data points^{3–5} show the CR spectral index as a function of the galactocentric distance obtained from Fermi-LAT data.

where $i = \nu, \gamma$ stands for neutrinos and gamma respectively, E_i and \hat{n}_i indicate the energy and arrival direction of the considered particles and $r_\odot = 8.5$ kpc is the position of the Sun. The total inelastic cross section in nucleon-nucleon collision, $\sigma(E)$, is given by:

$$\sigma(E) = 34.3 + 1.88 \ln(E/1\text{TeV}) + 0.25 \ln(E/1\text{TeV})^2 \text{ mb},$$

where E is the nucleon energy, while the spectra $F_i(E_i/E, E)$ of produced secondary particles are described (with 20% accuracy) by the analytic formulas given in Ref. 6. The constant A_i is equal to 1 for photons and $1/3$ for neutrinos, since the one flavour neutrino flux $\varphi_{\nu, \text{diff}}$ is obtained by summing over the production rates of ν_e and ν_μ in the sources, i.e.:

$$F_\nu(E_i/E, E) \equiv F_{\nu_\mu}(E_\nu/E, E) + F_{\nu_e}(E_\nu/E, E), \quad (2)$$

and then assuming flavour equipartition at Earth, as it is expected with good accuracy due to neutrino mixing, see e.g. Ref. 7. The gas density $n_H(\mathbf{r})$ is described as in Ref. 8; the heavy element contribution is included by assuming that the total mass of the interstellar gas is a factor 1.42 larger than the mass of hydrogen, as it is expected if the solar system composition is considered representative for the entire galactic disk.

Following Ref. 1, the CR nucleon flux is given as a function of position and nucleon energy by:

$$\varphi_{\text{CR}}(E, \mathbf{r}) = \varphi_{\text{CR}, \odot}(E) g(\mathbf{r}) h(E, \mathbf{r}) \quad (3)$$

where $\varphi_{\text{CR}, \odot}(E)$ represents the local flux,^a $g(r)$ is an adimensional function (normalized to one at the Sun position \mathbf{r}_\odot) introduced to describe the spatial distribution

^aIn this work, we use the symbol φ for angle-differential fluxes and Φ for angle-integrated fluxes.

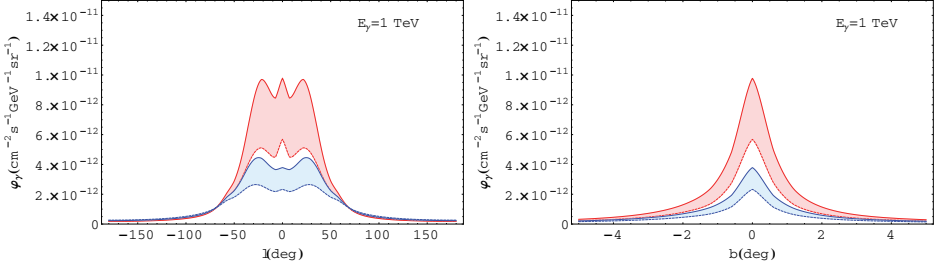


Fig. 2. The diffuse HE gamma-ray flux at $E_\gamma = 1$ TeV as a function of the Galactic longitude l (for $b = 0$) obtained by assuming that the CR spectrum is position-independent (blue lines) and by implementing CR spectral hardening in the inner Galaxy (red lines) as described by Eqs. (4), (8). Solid and dashed lines (in each group) are obtained by assuming that the CR spatial distribution follows that of SNR with smearing radius $R = 1$ kpc and $R = \infty$, respectively.

of CR while the function $h(E, \mathbf{r})$, given by:

$$h(E, \mathbf{r}) = \left(\frac{E}{\overline{E}} \right)^{\Delta(\mathbf{r})} \quad (4)$$

with $\overline{E} = 20$ GeV and $\Delta(\mathbf{r}_\odot) = 0$, introduces a position-dependent variation $\Delta(\mathbf{r})$ of the CR spectral index.

We describe the local CR nucleon flux $\varphi_{\text{CR},\odot}(E)$ according to the data driven parameterization given in Ref. 9 that relies as little as possible on theoretical assumptions. In the energy range of interest for the present analysis, that roughly corresponds to $E \simeq 10 \times E_\gamma \sim 10$ TeV when we consider photons with energy $E_\gamma \sim 1$ TeV, the total nucleon flux is lower than the broken-power law parameterization¹⁰ adopted in our previous calculation¹ by $\sim 12\%$. For neutrinos, we are interested at larger CR energies $E \simeq 20 \times E_\nu \sim 2$ PeV, as can be understood by considering that the astrophysical signal emerges from background components at $E_\nu \sim 100$ TeV in IceCube data. At these energies, the determination of the local flux is affected by relevant uncertainties and the total nucleon flux adopted in this work is reduced by a factor ~ 2 with respect to that given in Ref. 10.

The function $g(\mathbf{r})$ is determined by the distribution of the CR sources $f_S(\mathbf{r})$, that is assumed to follow the Supernova Remnants (SNR) number density parameterization given by Ref. 12, and by the propagation of CR in the Galactic magnetic field. Following Ref. 11, we define the function $g(\mathbf{r})$ as:

$$g(\mathbf{r}) = \frac{1}{\mathcal{N}} \int d^3x f_S(\mathbf{r} - \mathbf{x}) \frac{\mathcal{F}(|\mathbf{x}|/R)}{|\mathbf{x}|} \quad (5)$$

where \mathcal{N} is a normalization constant given by:

$$\mathcal{N} = \int d^3x f_S(\mathbf{r}_\odot - \mathbf{x}) \frac{\mathcal{F}(|\mathbf{x}|/R)}{|\mathbf{x}|} \quad (6)$$

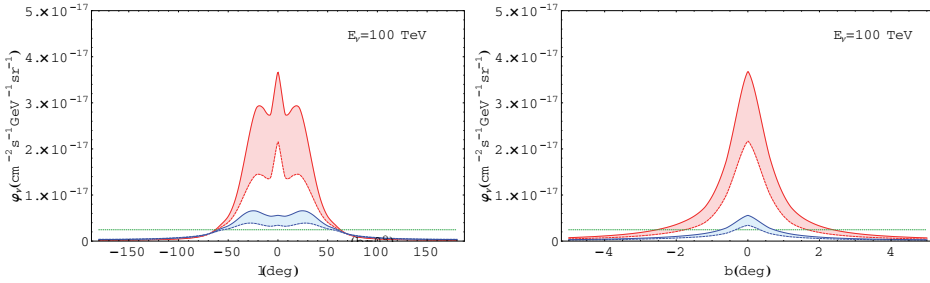


Fig. 3. The diffuse HE neutrino flux at $E_\nu = 100$ TeV as a function of the Galactic longitude l (for $b = 0$) obtained by assuming that the CR spectrum is position-independent (blue lines) and by implementing CR spectral hardening in the inner Galaxy (red lines) as described by Eqs. (4), (8). Solid and dashed lines (in each group) are obtained by assuming that the CR spatial distribution follows that of SNR with smearing radius $R = 1$ kpc and $R = \infty$, respectively.

while the function $\mathcal{F}(\nu)$ is defined as:

$$\mathcal{F}(\nu) \equiv \int_\nu^\infty d\gamma \frac{1}{\sqrt{2\pi}} \exp(-\gamma^2/2) \quad (7)$$

This kind of behaviour can be motivated as the solution of 3D isotropic diffusion equation with constant diffusion coefficient and stationary CR injection. In this context, the smearing parameter R represents the diffusion length $R = \sqrt{2D t_G}$, where D is the diffusion coefficient and t_G is the integration time.

The functions $g(\mathbf{r})$ calculated for different smearing radii R are shown as a function of the galactocentric distance by the black lines in the left panel of Fig. 1 where they are compared with the CR density at $E \simeq 20$ GeV and the γ -ray emissivity integrated above $E_\gamma = 1$ GeV (which is a proxy of the CR flux) obtained from Fermi-LAT data in Refs. 3, 4, 5. While we believe that the data show a clear trend as a function of r , we think that they still do not allow to discard any of the proposed curves. We thus consider the two extreme assumptions $R = 1$ kpc and $R = \infty$, corresponding to the thick black lines in Fig. 1, in order to encompass a large range of possibilities and to provide a conservative estimate of the uncertainty in the gamma-ray flux connected with different descriptions of the CR spatial distribution in the Galaxy.^b

The possibility of CR spectral hardening in the inner Galaxy is implemented by modelling the function $\Delta(\mathbf{r})$ in Eq. (4) as:

$$\Delta(r, z) = \Delta_0 \left(1 - \frac{r}{r_\odot} \right) \quad (8)$$

with $r_\odot = 8.5$ kpc, in galactic cylindrical coordinates. This choice is equivalent to what is obtained in Ref. 2 by considering a phenomenological CR propagation model

^bSince the assumed smearing length is larger than the thickness of the galactic disk, we neglect in both cases the variation of the CR flux along the galactic latitudinal axis. In other words, we assume $g(r, z) \simeq g(r, 0)$ in the disk, where we used galactic cylindrical coordinates.

characterized by radially dependent transport properties. The numerical parameter Δ_0 that physically corresponds to the difference between the CR spectral index at the Sun position, $\alpha_\odot \simeq 2.7$ at $E = 20$ GeV, and its value close to the galactic center, is taken as $\Delta_0 = 0.3$ since this assumption allows us to reproduce the trend with r observed in Refs. 3, 4, 5 for $r \leq 10$ kpc, as it is shown in the right panel of Fig. 1.^c In more external regions, the evidence for a variation of CR energy distribution is much weaker and we assume that $\Delta(r)$ is constant, as shown by the black solid line.

3. Results

The diffuse HE gamma-ray flux at $E_\gamma = 1$ TeV is plotted in Fig. 2 as function of the Galactic longitude (at the fixed latitude $b = 0$, left panel) and latitude (at the fixed longitude $l = 0$, right panel). Blue lines are obtained by assuming that the CR spectrum is independent from the position in the Galaxy (we refer to this in the following as the “standard” scenario) while red lines implement CR spectral hardening in the inner Galaxy. Solid and dashed lines in (each group) are obtained by assuming that the CR spatial distribution is described by the function $g(r)$ given in Eq. (5) with smearing radius equal to $R = 1$ kpc and $R = \infty$, respectively.

The angle-integrated gamma-ray flux is equal to $\Phi_\gamma = (7.0 - 8.0) \cdot 10^{-13} \text{ cm}^{-2} \text{ s}^{-1} \text{ GeV}^{-1}$ at 1 TeV in the standard scenario with upper and lower bounds corresponding to $R = 1$ kpc and $R = \infty$, respectively. The inclusion of CR hardening increases the integrated flux by $1.2 - 1.3$, the exact enhancement factor being dependent on the assumed CR spatial distribution. Even if the effect on the total flux is relatively small, CR hardening may be responsible for a much more significant increase of the gamma-ray flux in the central region $-60^\circ \leq l \leq 60^\circ$. We see indeed from Fig. 2 that the enhancement factor can be as large as ~ 2 in the direction of the Galactic center. This factor is larger than the uncertainty due to CR spatial distribution that can be conservatively estimated from the width of the coloured bands in the figure. Additional uncertainty sources are the normalization of the local CR flux at $E \sim 10 E_\gamma \sim 10$ TeV, the distribution of gas in the Galaxy, the hadronic interaction cross section, etc. All these are expected to produce a total error smaller than the difference between red and blue lines in the figure, suggesting that effects of CR hardening can be probed by TeV scale gamma-ray observations of the galactic central region. A detailed comparison of the obtained predictions with the observational data in the TeV domain by Argo-YBJ, HESS, Milagro and HAWC experiments is performed in Ref. 11.

Finally, the diffuse neutrino flux at $E_\nu = 100$ TeV is given as a function of the galactic longitude and latitude in Fig. 3 where we also show with a green line the isotropic astrophysical neutrino flux that is obtained from the six years HESE event rate observed by IceCube¹³. Our new calculations provide $\sim 40\%$ smaller neutrino

^cRefs. 4, 5 report the spectral index α_γ of gamma emission associated to π_0 decay. This is converted into the spectral index α of the parent CR by $\alpha_\gamma \simeq \alpha + 0.1$.

fluxes than what obtained in our previous work¹, as a combined consequence of the revised description of the local CR flux (which accounts for a factor ~ 2 reduction) and the inclusion of heavy element contribution to the galactic gas distribution (which is responsible for a $\sim 40\%$ enhancement). The angle-integrated neutrino flux is equal to $\Phi_\nu = (1.0 - 1.2) \cdot 10^{-18} \text{ cm}^{-2} \text{ s}^{-1} \text{ GeV}^{-1}$ at 100 TeV in the standard scenario and it is equal to $\sim 3 - 4\%$ of the isotropic astrophysical flux observed by IceCube. The inclusion of CR hardening increases the integrated flux by 1.5 – 1.8, the exact enhancement factor being dependent on the assumed CR spatial distribution. The effect is larger in the direction of the inner Galaxy where CR spectral hardening increases the predicted neutrino flux up to a factor ~ 6 , producing a visibly different angular distribution with respect to the standard scenario.

Acknowledgments

This work was partially supported by research grant number 2017W4HA7S “NAT-NET: Neutrino and Astroparticle Theory Network” under the program PRIN 2017 funded by Italian Ministero dell’Istruzione, dell’Università e della Ricerca (MIUR).

References

1. G. Pagliaroli, C. Evoli and F. L. Villante, JCAP **1611** (2016) no. 11, 004.
2. D. Gaggero, D. Grasso, A. Marinelli, A. Urbano and M. Valli, Astrophys. J. **815** (2015) no. 2, L25.
3. F. Acero *et al.* [Fermi-LAT Collaboration], Astrophys. J. Suppl. **223** (2016) no. 2, 26.
4. R. Yang, F. Aharonian and C. Evoli, Phys. Rev. D **93** (2016) no. 12, 123007.
5. M. Pothast, D. Gaggero, E. Storm and C. Weniger, JCAP **1810** (2018) no. 10, 045.
6. S. R. Kelner and F. A. Aharonian, Phys. Rev. D **78** (2008) 034013 Erratum: [Phys. Rev. D **82** (2010) 099901].
7. A. Palladino, G. Pagliaroli, F. L. Villante and F. Vissani, Phys. Rev. Lett. **114**, no. 17, 171101 (2015) doi:10.1103/PhysRevLett.114.171101 [arXiv:1502.02923 [astro-ph.HE]].
8. <http://galprop.stanford.edu/>.
9. H. P. Dembinski, R. Engel, A. Fedynitch, T. Gaisser, F. Riehn and T. Stanev, PoS ICRC **2017** (2018) 533.
10. M. Ahlers, Y. Bai, V. Barger and R. Lu, Phys. Rev. D **93**, no. 1, 013009 (2016).
11. M. Cataldo, G. Pagliaroli, V. Vecchiotti and F. L. Villante, arXiv:1904.03894 [astro-ph.HE].
12. D. A. Green, Mon. Not. Roy. Astron. Soc. **454** (2015) no. 2, 1517.
13. C. Kopper [IceCube Collaboration], PoS ICRC **2017**, 981 (2018).